

## FABRICATION OF POROUS SINTERED BODY USING SHAPE-CONTROLLED 316L STAINLESS STEEL POWDER BY HIGH-ENERGY BALL MILLING

In this study, 316L stainless steel powder was used to produce a porous body that could be used in a specific environment. In contrast to the existing method of producing filters using only spherical powders, we attempted to produce filters using plate- and needle-like powders and evaluated their performance. In the powder preparation step, the shape change of the powder was analyzed by changing the size of the stainless-steel balls used for ball milling. Then, the variations in properties of the sintered porous body caused by the ball size were investigated. As the average ball size decreased, the average particle size of the powder decreased. Moreover, the surface area and pore size of the porous body decreased. Additionally, when balls of different sizes were mixed, the porous body showed a mixture of coarse and fine pores.

*Keywords:* 316L stainless steel; porous body; ball milling; powder shape; sintering

### 1. Introduction

Currently, filters such as particulate matter and exhaust gases, that could be utilized in air purification have attracted considerable interest with increasing amounts of environmental pollutants. In addition, filters are used not only for mitigating environmental pollution but also in various fields such as separation processes in medicine and water purification, as well as in advanced fields such as biology, new materials, and semi-conductors.

With the increasing use of filters, they are applying in various environments, necessitating characteristics such as superheat resistance and corrosion resistance. The polymer used as the main material for conventional filters has low durability and cannot be used in harsh environments. By contrast, metallic materials such as stainless steel have excellent heat resistance, corrosion resistance, and strength. Moreover, compared to ceramic materials that are inherently brittle and difficult to deform, metal filters have the advantage of being reusable; therefore, they are attracting significant attention as filter materials [1]. Filters made of metallic materials have high porosity and high specific strength, which gives them several advantages. Additionally, due to their porosity, they exhibit functions such as sound absorption and vibration resistance through energy absorption, insulation via

internal pores, heat transfer ability through holes, and reaction acceleration owing to their large surface area [2-4].

Metal filters can be classified into powder, wire mesh, and fiber filters as different shapes of the material, and the porosity can be easily controlled by the change in the particle size of the powder or the diameter of the fiber. The powder-based filter is widely used because of its low manufacturing cost and simple manufacturing process; however, it has the disadvantages of low porosity and permeability compared to filters based on other materials. Therefore, several studies have been conducted to optimize the microstructure and porosity of this filter, particularly through the shape control of the powder.

We employed 316L stainless steel (STS316L) powder to fabricate the filter for use in harsh environments and reshaped the powder through ball milling to overcome the low porosity [5]. STS316L is a nonmagnetic material with high ductility and excellent workability due to its crystal structure [6-8]. STS316L contains molybdenum; therefore, it has improved corrosion resistance compared to other steel types. Further, by reducing the amount of carbon, hardness can be reduced and processability increases [9-11].

Plate- and needle-like powders were prepared by ball milling to fabricate metal filters with high specific surface area. We compared the particle size change of the powder and the

<sup>1</sup> SEOUL NATIONAL UNIVERSITY OF SCIENCE AND TECHNOLOGY, DEPARTMENT OF MATERIALS SCIENCE AND ENGINEERING, SEOUL, REPUBLIC OF KOREA

<sup>2</sup> SEOUL NATIONAL UNIVERSITY OF SCIENCE AND TECHNOLOGY, INSTITUTE OF POWDER TECHNOLOGY, SEOUL 01811, REPUBLIC OF KOREA

\* Corresponding author: [byun@seoultech.ac.kr](mailto:byun@seoultech.ac.kr)



characteristics of the porous body when the ball size changed. Characteristics such as porosity and specific surface area are affected by powder particle size [12]. In the case of plate- and needle-like powders, we evaluated the change in characteristics with particle size.

In this study, porous bodies were fabricated by controlling the shape through high-energy ball milling of the generally spherical STS316L powder. We evaluated the pore formation behavior by deriving the results based on the variation of ball size.

## 2. Experimental

### 2.1. Change in powder shape

The STS316L powder shown in Fig. 1 was used as the raw material powder in this study. The raw material powder exhibited a spherical shape and a particle size distribution of 5–8  $\mu\text{m}$ . STS316L powder was sealed with Ar gas in a grinding jar (STD 11, 500 ml) containing 250 ml of ethanol, and then high-energy ball milling was performed at a rotational speed of 300 rpm for 5 h. In the high-energy ball milling, stainless-steel balls with diameters of 4 and 8 mm were used as milling media, and the ball-to-powder weight ratio was 10:1. The plate-shaped powder was prepared in this way, and milling conditions were divided into “use only 4 mm balls,” “use only 8 mm balls” and “use 4 and 8 mm balls mixed in a weight ratio of 2.7:7.3” to analyze the particle size distribution of the plate-shaped powder when the ball size changes.

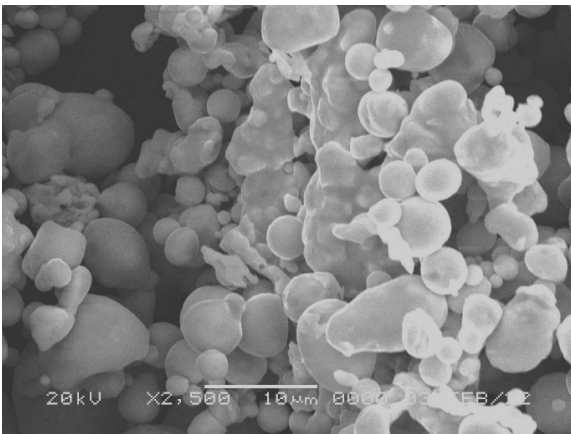


Fig. 1. SEM image of raw STS316L powder

### 2.2. Forming and sintering

Polyvinyl alcohol (PVA, DAEJUNG) with a polymerization degree of 500 was added as a binder to control the porosity and air permeability and obtain sufficient mold strength when manufacturing the porous body. PVA was mixed with distilled water in a ratio of 20 wt.% and stirred at 90°C for 2 h at a speed of 200 rpm with a magnetic bar on a hot plate and magnetic stirrer to prepare a binder.

The shape-changed powder and PVA binder were mixed in a weight ratio of 6:1, dried in a vacuum chamber for 24 h, and then pulverized. Subsequently, 1 g of the pulverized powder was filled into a 10 mm cylindrical mold and subjected to uniaxial pressing with a pressure of 30 MPa for 1 min.

Sintering was performed in a tubular gas furnace and in Ar atmosphere at a heating rate of 10°C/min. Thermal decomposition of the binder was performed at 400°C for 2 h, and the main sintering was performed at 950°C for 30 min.

### 2.3. Analysis

The size and shape changes of the powder by the variation of the ball size and microstructure of the porous sintered body produced from each powder were examined using a scanning electron microscope (SEM, Jeol – JSM-6300) and a field emission scanning electron microscope (FE-SEM, FEI – Apreo S Hivac). Then, the particle size of each powder was measured with a laser diffraction particle size analyzer (BECKMAN COUNTER – LS I3 320). Additionally, the various properties of porous bodies of each sintered body were measured through a pore-characterizing system (Micromeritics – AutoPore 9520).

## 3. Results and discussion

Fig. 2(a-c) shows the SEM images of the shape change of the powder by using different ball sizes. After ball milling for 5 h, the spherical raw material powder was completely changed into plate shape and needle shape. When only 4 mm balls were used, plate- and needle-shaped powders with small particle sizes were mainly observed. Moreover, when only 8 mm balls were used, plate-shaped powders with large particle sizes were mainly observed. In addition, the shape-changed powders showed a wide particle size distribution and aggregation with each other, which is a general characteristic of ductile metals. This was caused by the process of relatively fine powder agglomeration on the rough powder surface due to repeated crushing and welding by collisions between the ball and powder [13].

As shown in Fig. 2(d-f), when only 4 mm balls were used, the average particle size of the powder was 4.587  $\mu\text{m}$  and median particle size ( $d_{50}$ ) was 3.580  $\mu\text{m}$ ; when only 8 mm balls were used, the average particle size was 10.08  $\mu\text{m}$  and  $d_{50}$  was 7.109  $\mu\text{m}$ . Further, when 4 and 8 mm balls were mixed and used, the average size was 8.052  $\mu\text{m}$  and  $d_{50}$  was 5.995  $\mu\text{m}$ . Thus, the average and median particle size of the powder increased as more 8 mm balls were used. This is because the size of the empty space between the balls increases as their size increases, the contact area between the balls decreases, and the effect of crushing decreases.

4 mm balls and 8 mm balls were mixed in a weight ratio of 2.7:7.3 using the formula below.

$$X^* = \frac{f_L}{f^*}$$

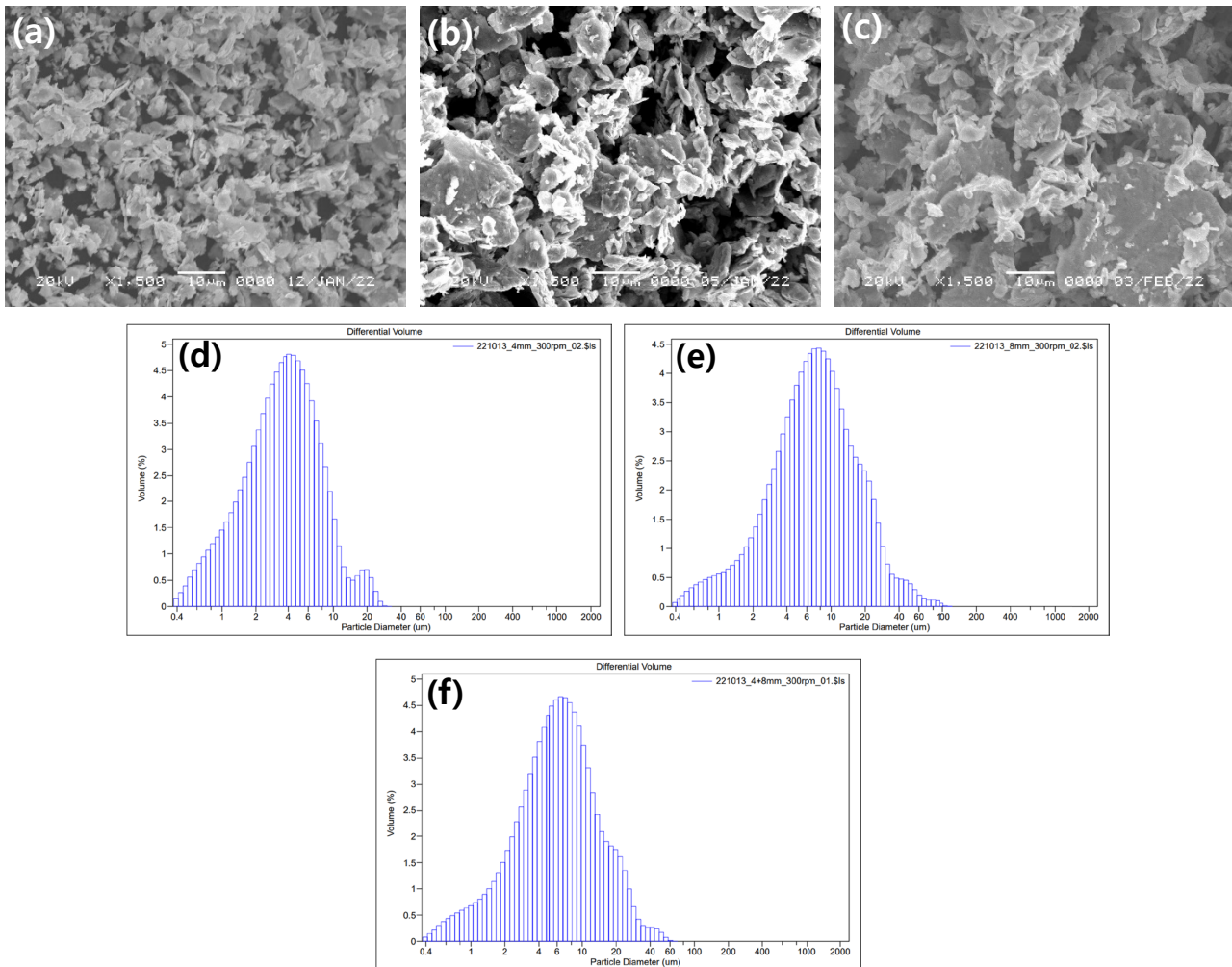


Fig. 2. SEM images and particle size analysis of STS316L powder milled for 5 h at 300 rpm: (a, d) using 4 mm, (b, e) 8 mm, and (c, f) (4 + 8) mm balls

$$f^* = f_L + f_S(1 - f_L)$$

$X^*$  is the optimal mixing ratio,  $f_L$  is the partial packing density of large particles,  $f_S$  is the partial packing density of small particles and  $f^*$  is the packing density in the optimal mixing [14]. In Fig. 2(d-f), the maximum powder size was 33.01  $\mu\text{m}$  when only 4 mm balls were used and 121.8  $\mu\text{m}$  when only 8 mm balls were used. And the maximum powder size was 69.62  $\mu\text{m}$  when 4 mm balls were mixed with 8 mm balls. The amount of powder that is less affected by crushing grows as the size of the balls increases, as does the empty space between the balls. Therefore, the empty space can be reduced and the maximum size of the powder can be reduced if small balls are mixed in proportion.

Fig. 3 shows the microstructure of the fabricated porous body. As observed in Fig. 3(a-c), thin, long, and irregular micropores of  $<10 \mu\text{m}$  were created owing to the plate-like powder. When only the 4 mm balls were used, relatively fine pores were distributed throughout, and when only the 8 mm balls were used, relatively few pores were formed on the surface. When 4 mm and 8 mm balls were mixed, the microstructure looked similar to the microstructure when only 8 mm balls were used, but the micropores were more distributed.

Fig. 3(d-f) shows cross sections of the porous sintered body in the direction parallel to the molding pressure direction, revealing that large micropores are formed under the influence of the aggregated powder. The porous body produced using 4 mm balls has relatively fine pores, and that created using 8 mm balls has relatively coarse pores. Additionally, both coarse and fine pores are distributed in the cross-sectional microstructure of the porous body produced by mixing 4 mm and 8 mm balls. As seen in TABLE 1, the porous body made using 8 mm balls had the largest porosity of 54.26%, while the total void area was the smallest at 0.574  $\text{m}^2/\text{g}$ . This is because the porous body prepared using 8 mm balls had the largest average pore diameter of 1071.1 nm. By contrast, the porous body made using 4 mm balls had the smallest average pore diameter of 537.2 nm and the largest total pore area of 1.251  $\text{m}^2/\text{g}$ . The total pore area and average pore size of the porous body could be efficiently controlled through the ball diameter.

The porous body produced by mixing 4 mm and 8 mm balls had a total pore area of 0.637  $\text{m}^2/\text{g}$  and an average pore diameter of 1006.3 nm. It has a larger total pore area and a smaller average pore diameter than the porous body made of 8 mm balls. This is the result of reducing the average particle size and maximum



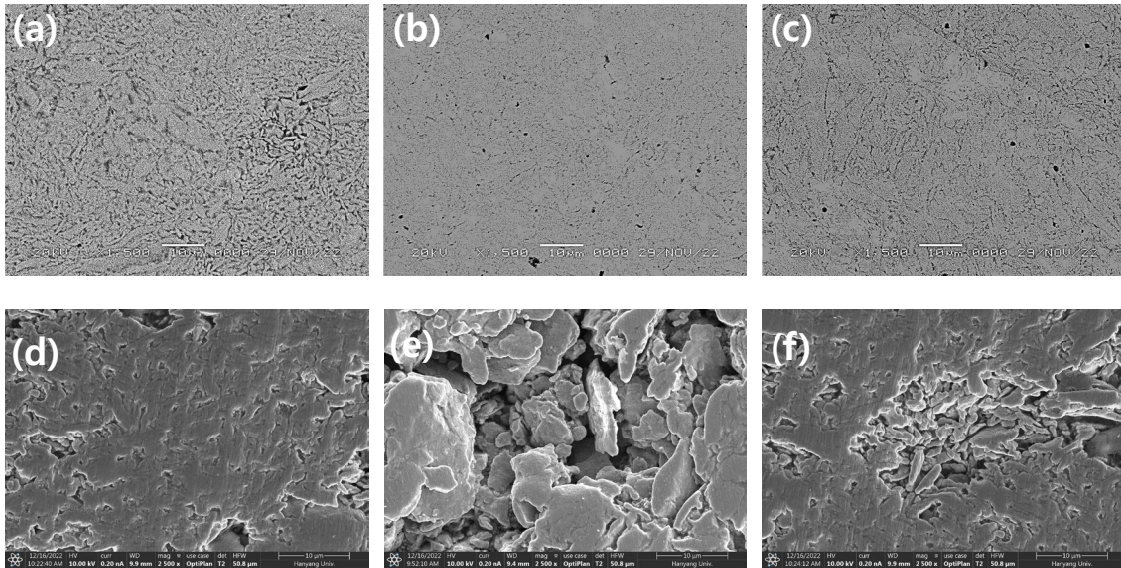


Fig. 3. SEM images (a-c) and FE-SEM cross-sectional images (d-f) of porous sintered body (30 MPa, 950°C, 30 min, Ar) with different ball sizes: (a, d) 4 mm, (b, e) 8 mm, (c, f) (4 + 8) mm

powder size by mixing 4 mm balls with 8 mm balls. Therefore, if changing the ball size to control the properties of the porous body is difficult, it is recommended to additionally mix balls with different diameters.

TABLE 1

Various properties of porous bodies

Ball Size (mm) \ Property	Total Pore Area (m <sup>2</sup> /g)	Average Pore Diameter (nm)	Porosity (%)
4	1.251	537.2	53.18
8	0.574	1071.1	54.26
4 + 8 (2.7:7.3)	0.637	1006.3	51.95

#### 4. Conclusions

In this study, plate-like and needle-like powder which can be applied in filters was fabricated using ball milling with 4 mm, 8 mm, and a mixture of 4 mm and 8 mm balls. Then, particle size distribution, microstructure, various properties of the porous bodies fabricated from each plate-like powder were investigated. The smaller the ball size, the smaller was the particle size of the powder formed, and many needle-shaped powder particles were observed in addition to the plate shape. In addition, the total pore area increased and fine pores were created when the porous body was formed. When large balls and small balls are mixed in an appropriate ratio in ball milling process, the formation of coarse powder can be suppressed that only occurs by using large balls. It also has the effect of decreasing the average pore size and increasing the pore area.

In summary, to effectively reduce the size of the powder, a smaller ball should be used, and the size of the ball should be appropriately adjusted to accurately control the total pore area and pore size. Especially, the powder size and properties of the porous body can be controlled through ball mixing.

#### Acknowledgments

This study was supported by the Research Program funded by SeoulTech (Seoul National University of Science and Technology).

#### REFERENCES

- [1] J. Qin, Q. Chen, C. Yang, Y. Huang, J. Alloys Compd **654**, 39-44 (2016).
- [2] J.D. Shim, J.Y. Byun, Korean J. Mater. Res. **25**, 155-164 (2015).
- [3] M.J. Lee, Y.J. Yi, H.J. Kim, M. Park, B.K. Kim, J.Y. Yun, J. Powder Mater. **25**, 415-419 (2018).
- [4] K.S. Kim, B.H. Kang, M. Park, J.Y. Yun, K.A. Lee, J. Powder Mater. **27**, 37-43 (2020).
- [5] N. Kurgan, R. Varol, Powder Technol. **201**, 242-247 (2010).
- [6] R.B. Song, J.Y. Xiang, D.P. Hou, J. Iron Steel Res. Int. **18**, 53-59 (2011).
- [7] G. Parr, A. Hanson, A.S.M. Materials Park, An Introduction to Stainless Steel, Ohio 1965.
- [8] A.R. Erickson, R.E. Wiech, A.S.M. Materials Park, Metals Handbook, Ohio 1994.
- [9] R. Fujisawa, M. Sakaiharu, Y. Kurata, Y. Watanabe, Corros. Eng. Sci. Technol. **40**, 244-248 (2013).
- [10] M. Imboby, K. Jiang, I. Chang, J. Micromech. Microeng. **18**, 115018 (2008).
- [11] K. Essa, F. Modica, M. Imboby, M.A. El-sayed, A. ElShaer, K. Jiang, H. Hassanin, Int. J. Adv. Manuf. Technol. **91**, 445-452 (2017).
- [12] J.G. Kim, J.I. Bang, Y.J. Kim, Y.H. Park, Korean J. Met. Mater. **51**, 857 (2013).
- [13] J.W. Song, H.S. Kim, H.M. Kim, T.S. Kim, S.J. Hong, J. Powder Mater. **17**, 302-311 (2010).
- [14] R.M. German, M.P.I.F. Princeton, Particle Packing Characteristics, New Jersey 1989.